Journal of Electroanalytical Chemistry 922 (2022) 116697

Contents lists available at ScienceDirect

Journal of Electroanalytical Chemistry

journal homepage: www.elsevier.com/locate/jelechem

Understanding the electrochemical hydrogenation of acetone on Pt single crystal electrodes

Dalila S. Mekazni, Rosa M. Arán-Ais *, Juan M. Feliu, Enrique Herrero

Instituto de Electroquímica, Universidad de Alicante, Apdo. 99, E-03080 Alicante, Spain

ARTICLE INFO

Keywords:
Electrocatalysis
Hydrogenation
Acetone
Pt(1 1 0)
Stepped surfaces
Supporting electrolyte

ABSTRACT

The heterogeneous upgrading of biomass by means of electrocatalytic hydrogenation is an attractive way to refine products for industrial and pharmaceutical purposes. Also, the efficient electrochemical reduction of carbonyl compounds can act as hydrogen vectors, and therefore energy vectors. In this manuscript, we render further fundamental insights into the electrochemical reduction of acetone as a model molecule of carbonyl compounds. The structural sensitivity of the reaction is demonstrated by using platinum single crystal electrodes with low Miller indices and stepped electrodes with (1 1 0) terraces and either (1 1 1) or (1 0 0) monoatomic steps. Among the basal planes, Pt(1 1 0) is the only one active for the electroreduction of acetone. The inclusion of (1 1 1) steps on the (1 1 0) terraces does not significantly alter the behavior of Pt(1 1 0), but increasing the (1 0 0) step density has been observed to decrease the activity. We attribute this different performance to a geometrical effect of the active sites. By using different supporting electrolytes, we have found that sulfate competes with acetone for the surface sites, thus modifying the adlayer interfacial structure and hampering acetone reactivity.

1. Introduction

The electrochemical hydrogenation of organic molecules has been the subject of upsurged interest over the past years. Further refinement of these biogenic compounds coming from biomass can be achieved under ambient conditions by applying a cathodic potential. In this sense, the traditional thermal methods employed and the hydrogen inputs coming from steam reforming of fossil fuels should be avoided, thus helping to reduce CO_2 emissions [1,2]. Besides the upgrading of biomolecules for industrial purposes, the efficient electrochemical hydrogenation of carbonyl compounds can act as hydrogen vectors, and therefore energy [3]. For instance, the acetone/isopropanol couple is a particular system of environmentally friendly organic liquids that selectively store hydrogen [4–6]. Being acetone the simplest ketone, fundamental insights into the electrochemical hydrogenation of its carbonyl functional group can render valuable knowledge into the refinement of biomass.

The electrochemistry of acetone has been previously studied on platinum [7–10], being both propane and 2-propanol the main reaction outcomes. The different product selectivity was firstly attributed to the existence of two types of adsorbed hydrogen, in which one of them is interstitial [7]. The history of the platinum electrode (anodic activation vs cathodized electrode) was also observed to play a role in the product selectivity. More recently, this diversity in the production of either propane or 2-propanol has been ascribed to the *surface sensitiveness* of acetone electroreduction [11], which is, in fact, related to the creation of different surface sites when platinum is anodically or cathodically corroded. Moreover, it has been shown that the hydrogenation of the carbonyl functional group not only depends on the surface geometry but also on the molecular structure of the reactant. For instance, acetone does not reduce on Pt(1 1 1) electrode, but acetophenone does due to a stronger interaction of the phenyl ring with this particular atomic arrangement [12].

Along these lines, the (1 1 0) structure of platinum has shown the best catalytic properties for the electroreduction of acetone [11]. After analyzing Pt[(n - 1)(1 1 1) × (1 1 0)] and Pt[(n + 1)(1 0 0) × (1 1 0)] electrodes, it was found that acetone reduction takes place on (1 1 0) steps, producing either 2-propanol or propane, respectively. This reaction is moreover rate determined by the proton-coupled electron transfer, thus being adsorbed hydrogen indispensable for the reduction to take place [9]. However, this also means that acetone and hydrogen compete for the adsorption sites, being the hydrogen evolution a parasitic reaction that hampers the hydrogenation of acetone.

* Corresponding author.
E-mail address: rosa.aran@ua.es (R.M. Arán-Ais).

https://doi.org/10.1016/j.jelechem.2022.116697
Received 18 May 2022; Received in revised form 30 July 2022; Accepted 10 August 2022
Available online 13 August 2022

Because of the inherent importance of surface structure and adsorption of species on the electroreduction of acetone, in this work, this reaction on platinum electrodes with low Miller index planes and stepped surfaces with (1 1 0) terraces and either (1 1 1) or (1 0 0) monoatomic steps has been studied. Different acidic supporting electrolytes have been used to design scenarios where a third species can compete for the adsorption sites or not. Moreover, the effect of acetone concentration has been also analyzed. We show that the active sites for the acetone electroreduction are those present in a row densely packed with Pt atoms separated by a distance of $2\sqrt{a}$ of the next row, being a the lattice parameter of the fcc structure of Pt.

2. Experimental section

The electrochemical setup and the preparation of Pt single crystal working electrodes have been previously described elsewhere [13,14]. In this work, the stepped electrodes used were those vicinal to the (1 1 0) pole, in the crystallographic [1 $\bar{1}$ 0] and [0 0 1] zones. These stepped surfaces have (1 1 0) terraces separated by monoatomic (1 1 1) and (1 0 0) steps, respectively. Before each measurement, the voltammetric profile of each electrode was recorded in the supporting electrolyte to check surface order and also that the solutions are free from any contamination. Experiments were carried out at room temperature in a three-electrode electrochemical cell de-aerated using argon (Air Liquide, N50). A Pt wire and reversible hydrogen electrode (RHE) were used as counter and reference electrodes, respectively. Cyclic voltammograms were recorded using an Autolab PGSTAT302N potentiostat in a hanging meniscus configuration. All the solutions were prepared using MilliQ water (Purelab flex, 18.2 MΩ) containing either sulfuric acid (Merck Suprapur, 96 %) or perchloric acid (Merck, for analysis 70–72 %) as the supporting electrolyte, and acetone (Sigma-Aldrich, ≥99,9 %) in different concentrations.

Fourier transform infrared (FTIR) spectroelectrochemical experiments were performed with a Nicolet Magna 850 spectrometer equipped with a MCT detector. The spectroelectrochemical cell was equiped with a prismatic CaF_2 window beveled at 60°. Experiments were performed at room temperature, with a reversible hydrogen electrode (RHE) and a platinum wire used as reference and counter electrodes, respectively. All the spectra were collected with a resolution of 8 cm^{-1} and are the average over 200 interferograms and p polarized light. They are presented as absorbance, according to $A = -\log(R/R_0)$ where R and R_0 are the reflectance corresponding to the single beam spectra obtained at the sample and reference potentials, respectively. Reference spectrum was taken at 0.8 V.

3. Results and discussion

In order to understand the electrochemical behavior of acetone on platinum electrodes, it is important to characterize its adsorption behavior, since the adsorption of the molecule governs its subsequent reactivity. Weak interactions or adsorption modes in unreactive configurations result in low activity. For this purpose, the voltammetric profiles in the presence of acetone with different concentrations have been recorded and compared to those obtained in its absence. The analysis seeks for oxidation or reduction currents and changes in the hydrogen adsorption profile of the electrode, which indicates the presence of strongly adsorbed species on the surface because of the specific interaction of acetone with the surface. Two different electrolytes will be used: 0.1 M perchloric acid and 0.1 M sulfuric acid, which differ in the interaction of the anion with the surface so that acetone adsorption can be compared in both scenarios. While perchlorate anions are not specifically adsorbed on the platinum surface, sulfate anions interact specifically with the surface after hydrogen desorption in a competitive process [15].

Fig. 1 shows the voltammetric profiles for the Pt(1 1 1) electrode in the two electrolytes in the presence and absence of 0.1 M acetone. Despite the high acetone concentration, the profiles are almost identical to those obtained in its absence. Moreover, no additional oxidation or reduction currents are observed, indicating that acetone is not undergoing a redox reaction. This result is in agreement with previous observations which neglected a rearrangement of the sulfate adlayer due to acetone adsorption [11,16]. Only very minor differences are detected between both supporting electrolytes. In perchloric acid solution, the peak at 0.8 V related to OH adsorption is less sharp, whereas in sulfuric acid the spike related to the phase transition of the sulfate layer is slightly displaced to higher potentials. We relate both changes to possible modification in the interfacial structure of the adlayer induced by the presence of acetone, which modifies the interactions of OH and sulfate with the surface. Anyhow, the results indicate that the interaction of acetone with the surface is weak because it does not alter the adsorption behavior of hydrogen or the anions (OH^-, in the case of perchloric acid, or sulfate). Moreover, the absence of any further reduction current besides the hydrogen evolution reaction (HER) points out that the interaction or contact of the acetone molecule with the Pt(1 1 1) surface occurs in a configuration that does not

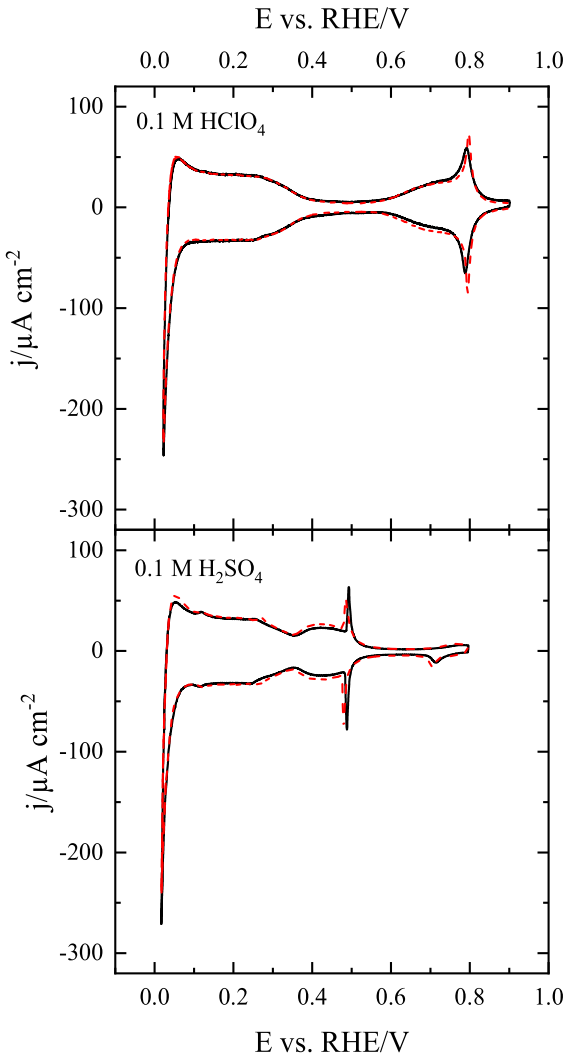

Fig. 1. Voltammetric profiles of the Pt(1 1 1) electrode in the presence (full black line) and the absence (dashed red line) of 0.1 M acetone in 0.1 M $HClO_4$ or 0.1 M H_2SO_4. Scan rate: 50 mV s^{-1}.

allow any reaction to take place [12]. This fact is supported by DFT calculations that showed the energetically unfavorable adsorption of acetone on Pt(1 1 1) and Pt(1 0 0) surfaces [11].

A different situation is found for the Pt(1 0 0) electrode (Fig. 2). In these voltammograms, the first two cycles are shown, because differences are observed between the first (full line), and the second (dashed line) and subsequent scans when it reaches a stationary behavior [11,16]. For this electrode, changes in the voltammetric profiles for acetone electroreduction when compared to those recorded in its absence are visible even for the lowest acetone concentration (10^{-3} M). In both electrolytes, a small oxidation process is observed at the upper potential limit. After the scan reversal, the currents measured for the hydrogen adsorption diminishes, indicating that some acetone-related species are adsorbed on the surface. The partial poisoning of the Pt(1 0 0) electrode was also noticed in the sulfuric electrolyte by [11,16] and has been recently ascribed to the dissociative adsorption of acetone on this surface geometry, giving rise to carbon monoxide and CH_x species that result in the deactivation of the electrode. The changes in the voltammetric profiles are more evident as concentration increases. For 0.01 M acetone and perchloric acid solutions, the voltammetric profile between 0.1 and 0.3 V during the first scan coincides with that obtained in the absence of acetone, indicating that no changes in the adsorbed layer on the electrode have occurred between 0.1 and 0.3 V. However, additional positive currents are observed from this later point and 0.5 V in the form of a peak. From the shape and charge involved in this peak, it can be assigned to an oxidative adsorption process of acetone on the Pt(1 0 0) surface. In this region, adsorbed hydrogen is being replaced by the adsorbed OH, which can catalyze the oxidative adsorption of acetone, in a similar way that it has been observed for methanol [17]. After the peak, the measured currents are those obtained typically for double layer charging processes, which indicates that this oxidative process is limited by the availability of free sites on the surface, a characteristic of adsorption processes. This oxidation is also incomplete, since above 0.6 V another oxidation process starts, which was also observed for the lowest concentration. For the concentrations which show significant oxidation currents above 0.6 V, oxidation currents are again observed at ca. 0.5 V in the negative scan direction. This potential is close to that of the peak observed in the positive scan direction. Thus, this current should be assigned to the readsorption of acetone-related species. This means that some adsorbed species have been oxidized at E > 0.6 V, and new free sites are available for the oxidative adsorption of acetone-derived species. From that point, the observed voltammetric profile in the hydrogen region corresponds to that measured on a partially blocked surface. Additionally, a very minor increase in the hydrogen evolution zone can be observed which may suggest very weak acetone reduction. In the second scan, the only significant difference is the disappearance of the peak at 0.4 V, which corroborates that this peak is related to an oxidative adsorption process, limited by the geometric availability of sites. For the highest acetone concentration, the peak associated with the oxidative adsorption of acetone during the first cycle is more intense and displaced to lower potentials, so that higher coverages are obtained. This results in lower oxidation currents at high potentials and a higher inhibition in the hydrogen adsorption process, as observed in the second scan. In sulfuric acid solutions, the qualitative behavior is the same, although, the presence of adsorbed sulfate hinders the oxidation of acetone at high potentials. However, the coverage of adsorbed species is very similar, because the hydrogen adsorption profile in the second cycle is very similar when the upper scan limit is set to 0.8 V (figure S1).

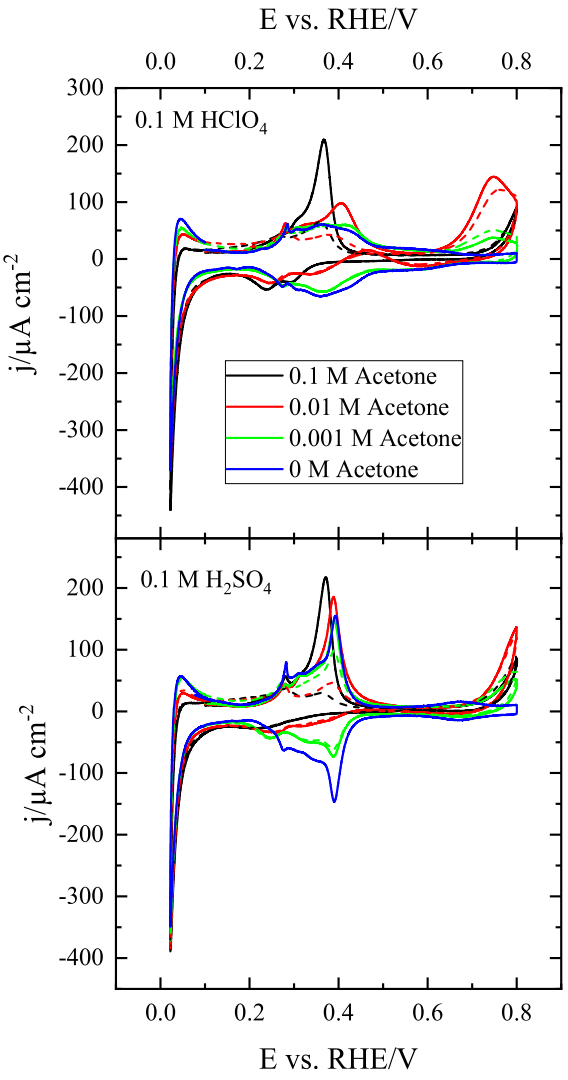

Fig. 2. Voltammetric profiles of the Pt(1 0 0) electrode in the presence of different acetone concentrations in 0.1 M $HClO_4$ or 0.1 M H_2SO_4. Full line: first scan; Dashed line: second scan. Scan rate: 50 mV s^{-1}.

Additional information on the behavior of acetone can be obtained using different upper potential limits for the voltammetry (Fig. 3). For this, a freshly annealed electrode is immersed in the cell at 0.1 V and two cycles are recorded using different upper potential limits between 0.5 and 0.9 V. In perchloric acid, the hydrogen adsorption profile in the negative scan of the first cycle and both scan directions of the second cycle is the same when the upper potential limited is between 0.5 and 0.7 V. This fact indicates that the oxidative adsorption of acetone forms stable adsorbed species on the surface in the potential region between 0 and 0.7 V and reaches a “saturation” coverage at 0.5 V, probably because of steric barriers within the adsorbed layer. In this sense, the C—C bond cleavage coming from this dissociative adsorption on Pt(1 0 0) terraces are thought to accumulate CH_x species and carbon monoxide on the electrode [16]. Similar conclusions were previously found for other organic molecules such as ethyl pyruvate [18]. For the higher upper limits, some acetone adsorbed species are being oxidized, together with acetone molecules from the bulk. As a result, in the negative scan direction oxidative currents are recorded at 0.5 V. The hydrogen adsorption profile for these scans shows higher currents. These observations are the consequence of the partial oxidation of the adsorbed acetone species during the oxidation wave centered at 0.8 V. The scenario is to some extent different in sulfuric acid solutions because the presence of specifically adsorbed sulfate hinders the processes related to acetone. Thus, for the upper limits between 0.5 and 0.7 V, the currents for hydrogen adsorption in the negative scan direction of the first cycle are larger than those in the

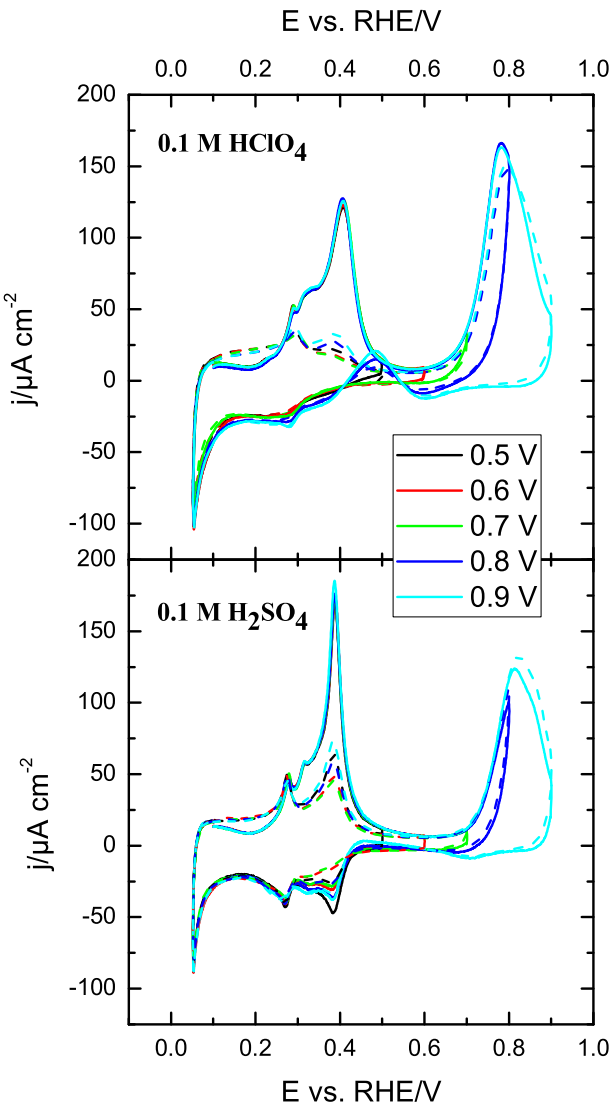

Fig. 3. Voltammetric profiles of the Pt(1 0 0) electrode in 0.01 M acetone in 0.1 M $HClO_4$ or 0.1 M H_2SO_4 with different upper potential limits. Full line: first scan; dashed line: second scan. Scan rate: 50 mV s^{-1}.

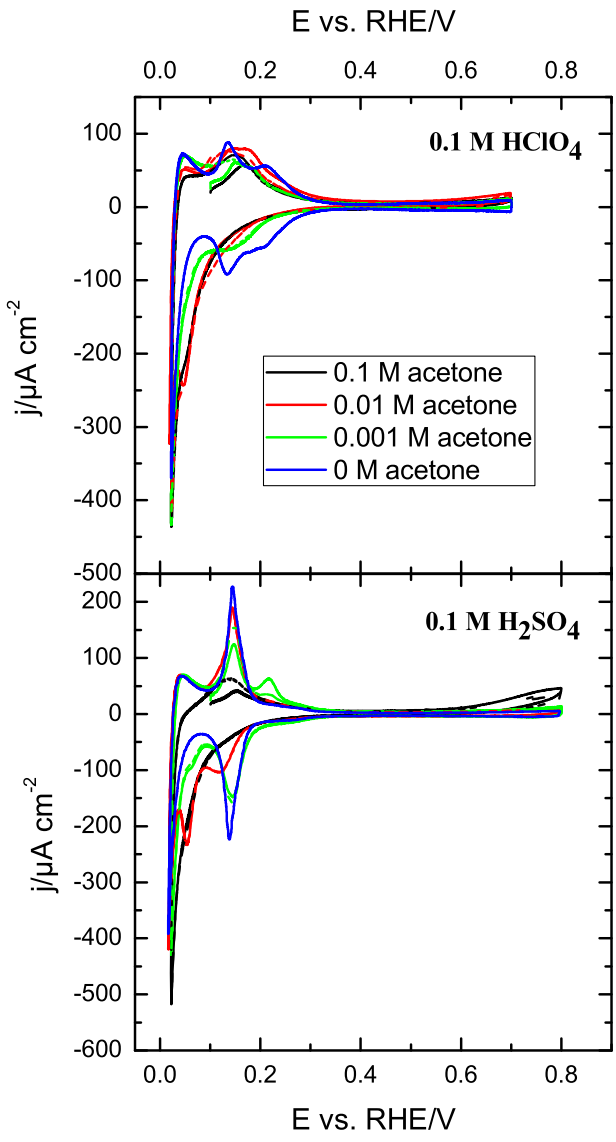

Fig. 4. Voltammetric profiles of the Pt(1 1 0) electrode in the presence of different acetone concentrations in 0.1 M $HClO_4$ or 0.1 M H_2SO_4. Full line: first scan; Dashed line: second scan. Scan rate: 50 mV s^{-1}.

second. It is clear then that the acetone adsorbed layer has not been completely formed during the first scan because the presence of adsorbed sulfate has hampered its formation. Additionally, when the upper potential limit is 0.9 V, some acetone adsorbed species are oxidized and desorbed, as happens in perchloric acid solution.

Among basal planes, the Pt(1 1 0) electrode is the only low index surface that shows significant reduction currents associated with acetone close to the hydrogen evolution region, as shown in Fig. 4. The unique properties of this atomic arrangement towards acetone electroreduction have been recently reported [11], highlighting that (1 1 0) steps on (1 1 1) and (1 0 0) terraces are the active sites for the hydrogenation of this molecule. In contrast to the Pt(1 1 1) electrode, where acetone does not adsorb, and the Pt(1 0 0) surface, where it oxidatively adsorbs, the adsorption of acetone on the Pt(1 1 0) electrode maintains the molecule intact either in the enolate or protonated form, depending on the applied potential. When the electrode is immersed in the solution at 0.1 V, acetone adsorption phenomena are already taking place because the currents between 0.1 and 0.3 V are smaller than those recorded in absence of acetone, even for the lowest concentration. If the adsorption of acetone species is related to the adsorption of OH, as proposed for the Pt(1 0 0) electrode, the onset for the OH adsorption process on the Pt(1 1 0) electrode is very close to 0.1 V, as indicated by the potential of zero total charge of this electrode (ca. 0.12 V) [19,20]. In the negative scan direction, hydrogen adsorption is partially blocked by the presence of acetone-derived species and at ca. 0.1 V, a reduction process appears superimposed on the currents related to the hydrogen evolution. In perchloric acid solutions, a significant increase in the negative currents is observed when the concentration is increased from 0.001 M to 0.01 M acetone, but from that point, the increase is almost negligible. Additionally, the hydrogen coverage measured in the following positive scan direction is higher, implying that some of the adsorbed species have been reduced. In sulfuric acid solutions, the qualitative behavior is similar. In fact, the difference in the hydrogen adsorption coverage between the positive and negative scan directions is clearer as the difference in current density for the peak at 0.13 V between positive and negative scan directions is very evident. The main difference is the presence of a

reduction peak centered at 0.06 V for the 0.01 M acetone solution. This type of peak has been already observed for other adsorbed species, such as hydroquinone [21] or catechol [22]. On the other hand, when comparing the reduction currents between sulfuric and perchloric acid solutions (figure S2), some differences are observed for the 0.01 M concentration. For a pure reduction process, without the interference of previously adsorbed species, it would have been expected that the currents in perchloric and sulfuric acid solutions were identical because, at the potentials at which the reduction of acetone takes place, anions have been completely desorbed and the hydrogen coverage is the same. However, this is not the case. For this acetone concentration, currents in sulfuric acid are slightly smaller with the appearance of the reduction peak at 0.06 V. Clearly, the difference is related to the formation of acetone-derived adlayer. The adlayer formed during the previous scan takes place actively in the reduction process and thus, the presence of sulfate, which adsorbs on the surface from 0.13 V leads to the formation of lower coverage, which is also pointed out by a lower blockage of the hydrogen region in sulfuric solution. Conversely, for the 0.1 M concentration, the reduction currents and the profiles in the hydrogen adsorption region are in both media are identical, implying that the acetone layer formed in the scans has reached similar coverage.

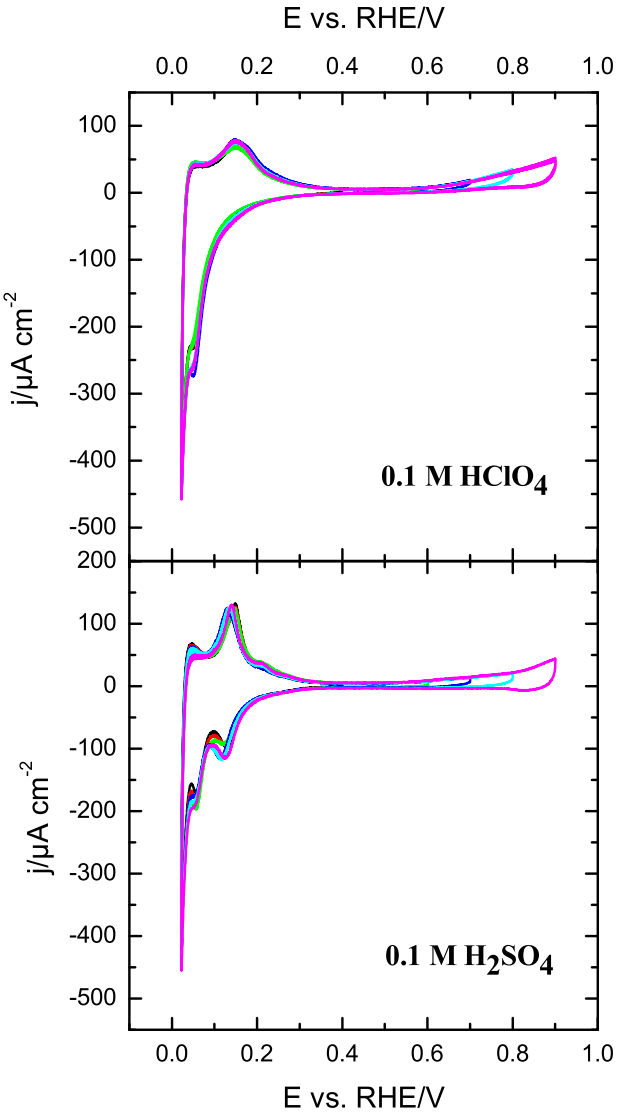

Fig. 5. Voltammetric profiles of the Pt(1 1 0) electrode in the presence of 0.01 M acetone in 0.1 M $HClO_4$ or 0.1 M H_2SO_4 with different upper potential limits. Scan rate: 50 mV s^{-1}.

If the acetone-derived adlayer is actively taking part in the reduction process, it is important to study the effect of the upper potential (Fig. 5), using the same procedure as that employed for the Pt(1 0 0) electrode. For the sulfuric acid solution, as the upper potential increases, the reduction peak at 0.06 V displaces to lower potential values, and its charge increases, which corroborates the previous hypothesis. In perchloric acid solutions, differences are minimal, indicating that, in the absence of the specific adsorption of anions, the adlayer is readily formed at potentials below 0.4 V. Thus, it can be concluded that for this electrode the adsorption process of acetone starts at low potentials and that there is a competition for the adsorption sites between acetone and sulfate and also with hydrogen at lower potentials.

In situ FTIR measurements on Pt(1 1 0) in perchloric acid electrolyte coincide with those previously reported [11]. Thus, the bands at 2965 and 2877 cm^{-1} correspond to the asymmetric and symmetric stretching vibrations of the methyl group of 2-propanol. In addition, a band at 2936 cm^{-1} is also observed, which can be assigned to propane asymmetric and symmetric stretching vibrations of the methyl group (figure S3).

Since the Pt(1 1 0) electrode is the only one among the basal planes on which acetone reduction takes place, it is important to know how the actual surface structure of this plane affects the reduction. It has been shown that acetone hydrogenation only takes place at the step sites of both Pt[(n-1)(1 1 1)×(1 1 0)] and Pt[(n + 1)(1 0 0)×(1 1 0)] electrodes [11,16]. However, the product distribution is significantly influenced by the nature of the terrace since propane is generated at the steps sites of Pt[(n)(1 0 0)×(1 1 0)] electrodes whereas 2-propanol is formed at the steps of Pt[(n-1)(1 1 1)×(1 1 0)] surfaces. Here, the behavior of stepped surface containing (1 1 0) symmetry terrace sites and (1 1 1) steps (with Miller indexes Pt(2n-1,2n-1,1), where n is the atomic terrace length) or (1 0 0) steps (with Miller indexes Pt(n,n-1,0)) is analyzed. Fig. 6 shows the results for both series of stepped surfaces in perchloric acid solution. The qualitative behavior in sulfuric acid solutions (figure S3) follows the same trends. Differences in the behavior can be observed depending on the step symmetry. For clarity, an enlargement of the acetone reduction region has been added as an inset to the graphs. For the surfaces containing (1 1 1) steps, a diminution of the activity for the reduction is observed, although, for the surface with the highest step density, the Pt(3 3 1) electrode, significant reduction currents are still measured. This surface is the so-called turning point in the [$1\bar{1}0$] crystallographic zone because it can be considered as a surface containing 2 atom-wide (1 1 0) terraces separated by a (1 1 1) monoatomic step or 2 atom-wide (1 1 1) terraces separated by (1 1 0) monoatomic steps. This result agrees with the observed behavior of the stepped surfaces containing (1 1 1) terraces and (1 1 0) steps, in which the activity for the acetone reduction reaction is proportional to the (1 1 0) step density [11]. On the other hand, for the surfaces containing (1 0 0) steps, which belong to the stereographic zone [0 0 1], a small diminution is observed as the step density increases, although for the Pt(2 1 0) electrode, which is the turning point in this series, the reduction currents are significantly smaller and largely suppressed for the higher acetone concentration.

As previously mentioned, acetone dissociatively adsorbs on the Pt (1 0 0) terrace sites as CO/CH_x species, leading to the deactivation of the electrode. However, this oxidative adsorption does not take place on (1 0 0) step sites, meaning that more than two neighboring atoms with (1 0 0) symmetry are needed for the dissociative adsorption of acetone [16]. Therefore, the different activity for the two series is not due to the poisoning of the Pt[n(1 1 0)×(1 0 0)] surfaces, but can be related to the different geometry of the step sites, as shown in Fig. 7. The Pt(1 1 0) surface can be even considered as a step surface

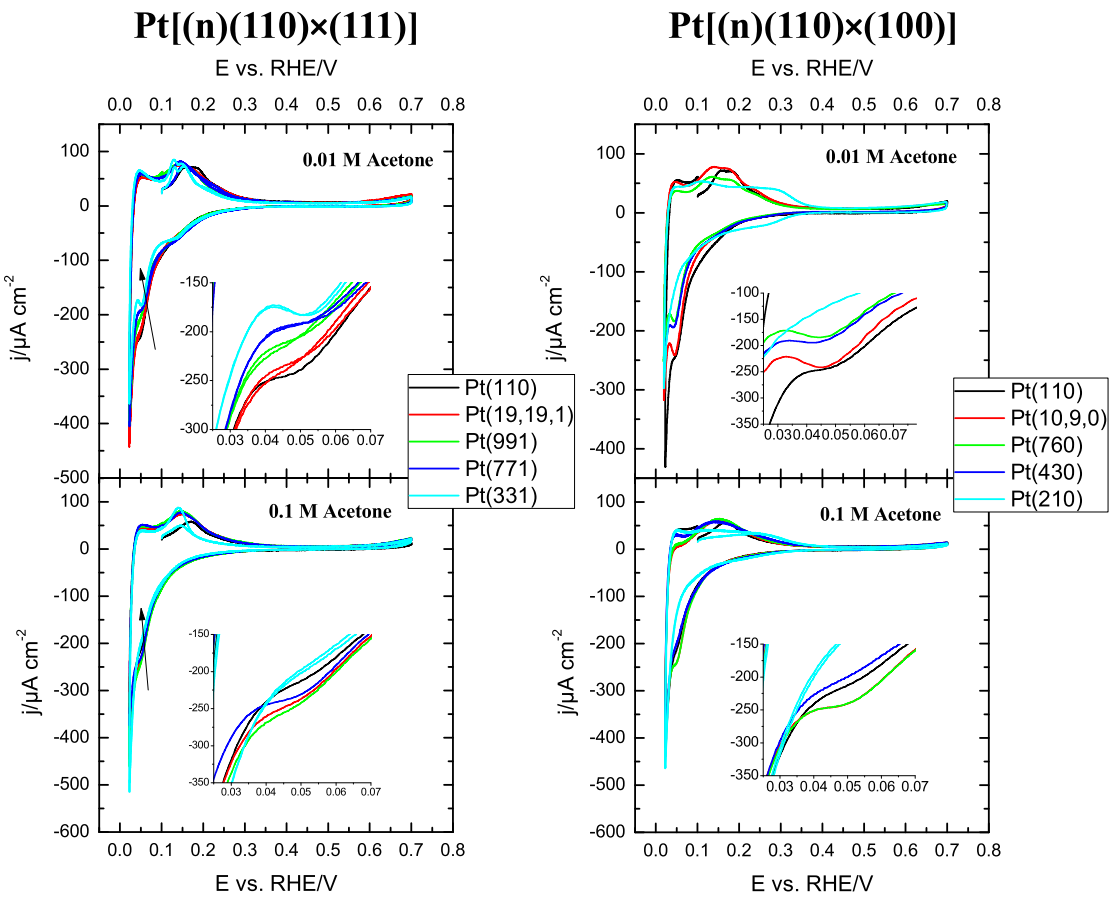

Fig. 6. Voltammetric profiles of the Pt(n,n-1,0) and Pt(2n-1, 2n-1,1) stepped surfaces in 0.1 M $HClO_4$ with different acetone concentrations. Insets show magnification of the acetone reduction peak. Scan rate: 50 mV s^{-1}.

with two atom-wide (1 1 1) terraces and a (1 1 1) monoatomic step. Then, the activity can be linked to the presence of a row of atoms densely packed Pt atoms separated by a distance of $2\sqrt{a}$ of the next row, being a the lattice parameter of the fcc structure of Pt. This row is shown in Fig. 7 enclosed in a box. The introduction of (1 1 1) steps, only reduces the number of these rows and for this reason, the activity only shows a small diminution, as can be seen in the hard-sphere model of (5 5 1) surface (Fig. 7). Also, this row of atoms, which is also present on the (1 1 0) steps on the (1 1 1), terraces explains the activity found for this series of surfaces. On the other hand, (1 0 0) steps on the (1 1 0) terraces run perpendicular to these rows, as shown for the (3 1 0) surface, breaking the active row. Since acetone is a molecule that needs more than one site for the adsorption, the presence of the step diminishes the number of contiguous sites and, for the Pt(2 1 0) surface, the number of contiguous sites on the surface with the appropriate symmetry is only one and the reduction of acetone cannot take place.

4. Conclusions

In this paper, we have investigated the electrochemical hydrogenation of acetone on platinum single crystal electrodes using acidic supporting electrolytes with a different interplay of the anion with the surface, and several acetone concentrations. The Pt(1 1 1) electrode shows no interaction with acetone and does not undergo a redox reaction. However, we noticed a plausible change in the interactions of OH and sulfate with the surface caused by the presence of acetone, thus pointing out a modification in the interfacial structure of the adlayer. On the contrary, Pt(1 0 0) presents a different behavior in which the molecule of acetone dissociatively engages with the surface, displaying oxidative currents above 0.5 V that coincides with the presence of adsorbed OH. It has been observed that although the coverage reached by acetone-related species is similar in both perchloric and sulfuric acid, the presence of adsorbed sulfate hampers acetone oxidation at high potentials. Apart from the oxidative adsorption on Pt(1 0 0) surface, acetone does not experience a significant reduction on this electrode. For Pt(1 1 0), clear reduction peaks were observed. We propose that the interaction of acetone with the surface is related to OH adsorption (ca. 0.12 V). Therefore, the presence of sulfate leads to lower acetone coverages and slightly smaller reduction currents when compared with those recorded in the perchloric acid electrolyte. The behavior of stepped surfaces containing (1 1 0) symmetry terrace sites and either (1 1 1) or (1 0 0) steps has been illustrated. Pt[n(1 1 0)×(1 1 1)] electrodes display a minor activity diminution as the step density increases. On the contrary, reduction currents are minimal for Pt[n(1 1 0)×(1 0 0)] surfaces when the step density increases. We conclude that the active sites for the electroreduction of acetone are those present in a row densely packed with Pt atoms separated by a distance of $2\sqrt{a}$ of the next row, being a the lattice parameter of the fcc structure of Pt. Therefore, acetone reduction only takes place when this geometrical requirement is fulfilled.

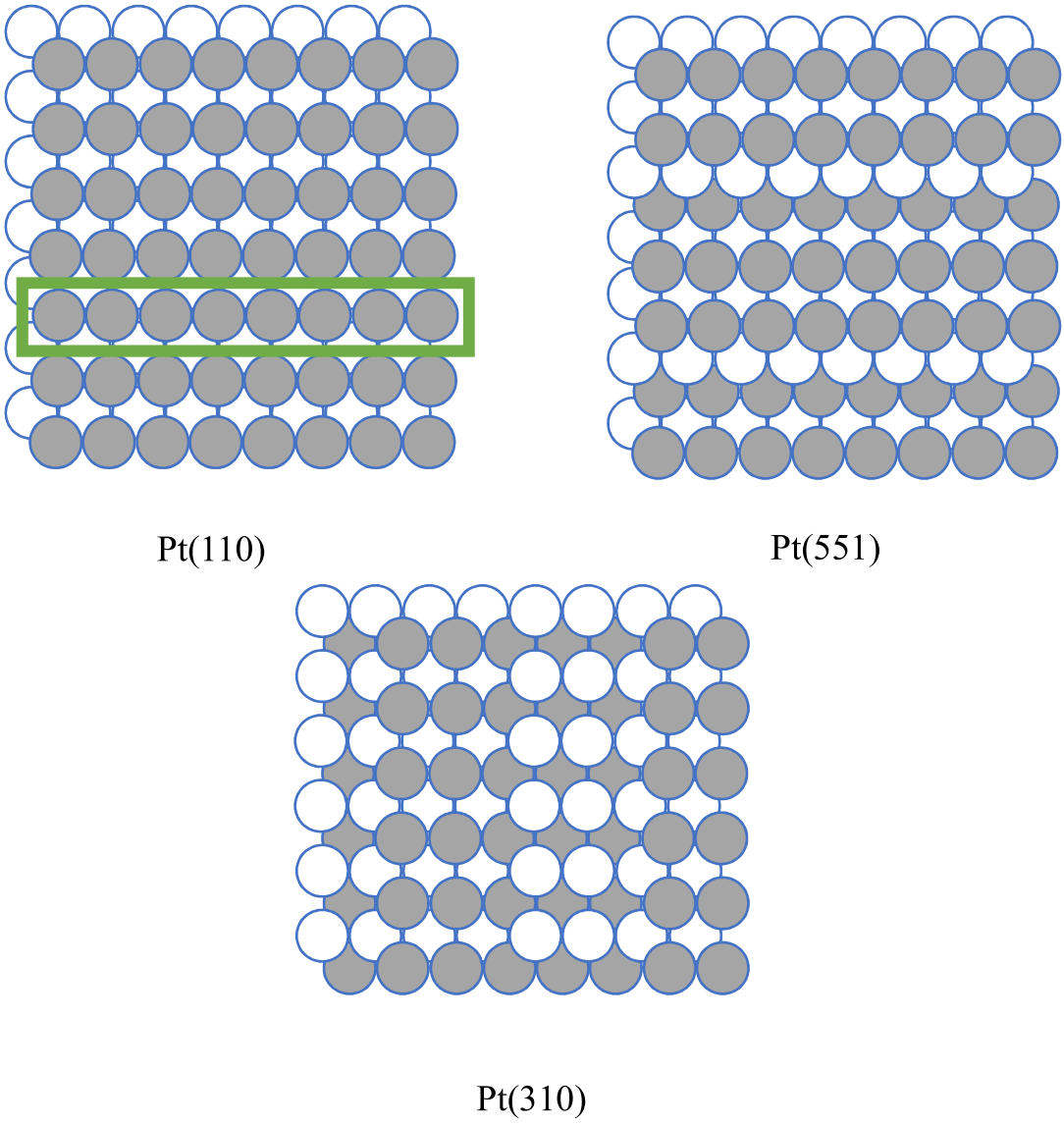

Fig. 7. Hard sphere models for the Pt(110), Pt(551), and Pt(310) surfaces. The green box indicates the row of atoms active for the reduction of acetone.

Data availability

Data will be made available on request.

Declaration of Competing Interest

The authors declare that they have no known competing financial interests or personal relationships that could have appeared to influence the work reported in this paper.

Acknowledgments

This research was funded by Ministerio de Ciencia e Innovación (Spain) grant number PID2019-105653 GB-I00), Generalitat Valenciana (Spain) grant number PROMETEO/2020/063. RMAA. acknowledges the financial support from Generalitat Valenciana (CDEIGENT/2019/018).

Appendix A. Supplementary data

Supplementary data to this article can be found online at https://doi.org/10.1016/j.jelechem.2022.116697.

References

[1] R.S. Weber, J.E. Holladay, Modularized Production of Value-Added Products and Fuels from Distributed Waste Carbon-Rich Feedstocks, Engineering. 4 (2018) 330–335, https://doi.org/10.1016/j.eng.2018.05.012.
[2] U. Sanyal, J. Lopez-Ruiz, A.B. Padmaperuma, J. Holladay, O.Y. Gutiérrez, Electrocatalytic Hydrogenation of Oxygenated Compounds in Aqueous Phase, Org. Process Res. Dev. 22 (2018) 1590–1598, https://doi.org/10.1021/acs.oprd.8b00236.
[3] F. Valentini, A. Marrocchi, L. Vaccaro, Liquid Organic Hydrogen Carriers (LOHCs) as H-Source for Bio-Derived Fuels and Additives Production, Adv. Energy Mater. n/a 12 (13) (2022), https://doi.org/10.1002/aenm.202103362.
[4] P. Hauenstein, D. Seeberger, P. Wasserscheid, S. Thiele, High performance direct organic fuel cell using the acetone/isopropanol liquid organic hydrogen carrier system, Electrochem. Commun. 118 (2020), https://doi.org/10.1016/j.elecom.2020.106786 106786.
[5] M. Brodt, K. Müller, J. Kerres, I. Katsounaros, K. Mayrhofer, P. Preuster, P. Wasserscheid, S. Thiele, The 2-Propanol Fuel Cell: A Review from the Perspective

of a Hydrogen Energy Economy, Energy Technol. 9 (2021) 2100164, https://doi.org/10.1002/ente.202100164.
[6] C. Stumm, M. Kastenmeier, F. Waidhas, M. Bertram, D.J.S. Sandbeck, S. Bochmann, K.J.J. Mayrhofer, J. Bachmann, S. Cherevko, O. Brummel, J. Libuda, Model electrocatalysts for the oxidation of rechargeable electrofuels - carbon supported Pt nanoparticles prepared in UHV, Electrochim. Acta. 389 (2021), https://doi.org/10.1016/j.electacta.2021.138716 138716.
[7] X. de Hemptinne, K. Schunck, Electrochemical reduction of acetone. Electrocatalytic activity of platinized platinum, Trans. Faraday Soc. 65 (1969) 591–597, https://doi.org/10.1039/TF9696500591.
[8] C. Wagner, Considerations on the mechanism of the hydrogenation of organic compounds in aqueous solutions on noble metal catalysts, Electrochim. Acta. 15 (1970) 987–997, https://doi.org/10.1016/0013-4686(70)80039-1.
[9] C.J. Bondue, M.T.M. Koper, A mechanistic investigation on the electrocatalytic reduction of aliphatic ketones at platinum, J. Catal. 369 (2019) 302–311, https://doi.org/10.1016/j.jcat.2018.11.019.
[10] B. Bänsch, T. Härtung, H. Baltruschat, J. Heitbaum, Reduction and oxidation of adsorbed acetone at platinum electrodes studied by DEMS, J. Electroanal. Chem. Interfacial Electrochem. 259 (1989) 207–215, https://doi.org/10.1016/0022-0728(89)80048-8.
[11] C.J. Bondue, F. Calle-Vallejo, M.C. Figueiredo, M.T.M. Koper, Structural principles to steer the selectivity of the electrocatalytic reduction of aliphatic ketones on platinum, Nat. Catal. 2 (2019) 243–250, https://doi.org/10.1038/s41929-019-0229-3.
[12] C.J. Bondue, M.T.M. Koper, Electrochemical Reduction of the Carbonyl Functional Group: The Importance of Adsorption Geometry, Molecular Structure, and Electrode Surface Structure, J. Am. Chem. Soc. 141 (2019) 12071–12078, https://doi.org/10.1021/jacs.9b05397.
[13] J. Clavilier, D. Armand, S.G. Sun, M. Petit, Electrochemical adsorption behaviour of platinum stepped surfaces in sulphuric acid solutions, J. Electroanal. Chem. Interfacial Electrochem. 205 (1986) 267–277, https://doi.org/10.1016/0022-0728(86)90237-8.
[14] R.M. Arán-Ais, M.C. Figueiredo, F.J. Vidal-Iglesias, V. Climent, E. Herrero, J.M. Feliu, On the behavior of the Pt(1 0 0) and vicinal surfaces in alkaline media, Electrochim. Acta. 58 (2011) 184–192, https://doi.org/10.1016/j.electacta.2011.09.029.
[15] N. Garcia-Araez, V. Climent, P. Rodriguez, J.M. Feliu, Thermodynamic analysis of (bi)sulphate adsorption on a Pt(111) electrode as a function of pH, Electrochim. Acta. 53 (2008) 6793–6806, https://doi.org/10.1016/j.electacta.2007.12.086.
[16] C.J. Bondue, Z. Liang, M.T.M. Koper, Dissociative Adsorption of Acetone on Platinum Single-Crystal Electrodes, J. Phys. Chem. C. 125 (2021) 6643–6649, https://doi.org/10.1021/acs.jpcc.0c11360.
[17] D.S. Mekazni, R.M. Arán-Ais, A. Ferre-Vilaplana, E. Herrero, Why methanol electro-oxidation on platinum in water takes place only in the presence of adsorbed OH, ACS Catal. 12 (2022) 1965–1970, https://doi.org/10.1021/acscatal.1c05122.
[18] O.A. Hazzazi, S.E. Huxter, R. Taylor, B. Palmer, L. Gilbert, G.A. Attard, Electrochemical studies of irreversibly adsorbed ethyl pyruvate on Pt{hkl} and epitaxial Pd/Pt{hkl} adlayers, J. Electroanal. Chem. 640 (2010) 8–16, https://doi.org/10.1016/j.jelechem.2009.12.026.
[19] J. Souza-Garcia, V. Climent, J.M. Feliu, Voltammetric characterization of stepped platinum single crystal surfaces vicinal to the (110) pole, Electrochem. Commun. 11 (2009) 1515–1518, https://doi.org/10.1016/j.elecom.2009.05.044.
[20] J. Souza-Garcia, C.A. Angelucci, V. Climent, J.M. Feliu, Electrochemical features of Pt(S)[n(110) × (100)] surfaces in acidic media, Electrochem. Commun. 34 (2013) 291–294, https://doi.org/10.1016/j.elecom.2013.07.007.
[21] M. Rodríguez-López, J. Solla-Gullón, E. Herrero, P. Tuñón, J.M. Feliu, A. Aldaz, A. Carrasquillo, Electrochemical Reactivity of Aromatic Molecules at Nanometer-Sized Surface Domains: From Pt(hkl) Single Crystal Electrodes to Preferentially Oriented Platinum Nanoparticles, J. Am. Chem. Soc. 132 (7) (2010) 2233–2242.
[22] M. Rodríguez-López, E. Herrero, V. Climent, A. Rodes, A. Aldaz, J.M. Feliu, A. Carrasquillo, Size-dependent and step-modulated supramolecular electrochemical properties of catechol-derived adlayers at pt(hkl) surfaces, Langmuir. 29 (42) (2013) 13102–13110.